JOURNAL OF SOLID STATE CHEMISTRY 77, 281–292 (1988)

Strontianite–Aragonite Solid Solutions $Sr_xCa_{1-x}CO_3$: Effect of Composition on the Orthorhombic–Rhombohedral Phase Transition and the Conversion to Oxide Solid Solutions $Sr_xCa_{1-x}O$

BICE FUBINI

Dipartimento di Chimica Inorganica, Chimica Fisica e Chimica dei Materiali, Università di Torino, Via P. Giuria 9, 10125 Torino, Italy

FRANCESCO DI RENZO*

Dipartimento di Chimica Industriale ed Ingegneria Chimica, Politecnico di Milano, Piazza L. da Vinci 32, 20133 Milano, Italy

AND FRANK S. STONE

School of Chemistry, University of Bath, Bath BA2 7AY, England

Received March 31, 1988

The conversion of orthorhombic $Sr_xCa_{1-x}CO_3$ solid solutions to $Sr_xCa_{1-x}O$ has been studied by thermal analysis and X-ray diffraction. The decomposition occurs in two stages. In the first stage, occurring at 950–1150 K in N_2, the cations demix to produce CaO and leave a Sr-enriched carbonate phase. In the second stage (1150–1350 K) the residual carbonate decomposes and the cations remix to form the oxide solid solution. By heating in CO_2, thereby displacing decomposition to above 1250 K, the orthorhombic–rhombohedral phase transition characteristic of these carbonates has been studied over the whole range $x = 0 \rightarrow 1$. The transition temperature (T_{tr}) increases progressively with x. For the Sr-enriched carbonate obtained after the first stage of decomposition in N_2, T_{tr} is independent of the initial composition and close to that for $SrCO_3$. ΔH for the transition, however, is less than that expected for well-crystallized $SrCO_3$, suggesting that the demixed carbonate is partly amorphous.

Introduction

Alkaline earth carbonates are well known to exhibit solid solution formation to some extent, but the composition interval in which they can be obtained as such by chemical preparation is not well defined. Most of the work on the binary and ternary solid solutions has been performed on mineral samples with mainly geological interests in mind (*1*). However, the solid state chemistry and thermal decomposition to oxides as separate phases or in solid solution has been thoroughly studied in the case of dolomite, $Mg_{0.5}Ca_{0.5}CO_3$ (*2–10*), and to a limited extent in the case of $CaCO_3$–$SrCO_3$ (*11–15*) and $SrCO_3$–$BaCO_3$ (*16*). Interest in the decomposition of mixed carbonates has

* Present address: Ecole Nationale Superieure de Chimie de Montpellier, CNRS UA 418, 8 Rue de l'Ecole Normale, 34075 Montpellier, France.

0022-4596/88 $3.00

also been raised by a recent report that at intermediate states of decomposition very reactive surface arrangements of potential interest in catalysis can be found (*17*).

Our work in this field (*13–15*) has involved the chemical preparation and characterization of $CaCO_3$–$SrCO_3$ solid solutions ($Sr_xCa_{1-x}CO_3$), together with some studies of thermal decomposition. Decomposition in inert gas flow was found to occur in two separate stages, as happens when dolomite is decomposed in CO_2. However, in contrast with what is observed with dolomite, the final product from $Sr_xCa_{1-x}CO_3$ is an oxide solid solution (*13, 14*).

There has been much previous work on the end members, $CaCO_3$ and $SrCO_3$. The thermal decomposition of pure $CaCO_3$ (as calcite) has been the object of a great deal of research (*2, 3*), latterly from the kinetic point of view in particular (*18–20*); some recent work has also appeared on the heat of decomposition (*21*). The decomposition of pure $SrCO_3$ has also been investigated (*22, 23*). Both $CaCO_3$ and $SrCO_3$ have orthorhombic and rhombohedral polymorphs. At normal temperature the stable form of $CaCO_3$ is the rhombohedral phase (calcite) whereas the stable modification for $SrCO_3$ is the orthorhombic polymorph (strontianite). Orthorhombic $CaCO_3$ (aragonite) is widely found in nature (*24*), and can also be prepared under laboratory conditions; on heating it is irreversibly converted into calcite (*25*). Orthorhombic $SrCO_3$ (strontianite) also undergoes a phase transition into a rhombohedral form upon heating, but the transition is reversible and the rhombohedral form cannot be quenched (*26*). This phase transition has been investigated by Rao and Mehrotra (*27*) and has also been proposed as a DTA standard (*28, 29*).

The orthorhombic–rhombohedral transition in $Sr_xCa_{1-x}CO_3$, however, has not to our knowledge been previously investigated. The occurrence of orthorhombic aragonite–strontianite solid solutions has been reported by several authors (*13, 30, 31*). The corresponding rhombohedral solid solutions are also known to exist, but there is only limited information (*32, 33*) on the range of composition in which they can be found.

The aim of the present paper is to report a thorough investigation under both N_2 and CO_2 flow of the thermal decomposition of chemically prepared aragonite–strontianite solid solutions and the evaluation of the heat of decomposition as a function of the composition. The stabilizing effect of Sr ions on the carbonate structure has already been described in a previous paper (*15*). The orthorhombic–rhombohedral transition in the solid solutions has also been investigated, with particular attention being given to the influence of composition upon the temperature at which the phase transition occurs, its reversibility, and the heat released in the transition itself. Because of the irreversibility of the transition in a wide range of compositions the quenching of some rhombohedral solid solutions is possible and, consequently, the lattice parameters can be evaluated. The characteristics of the transition in the half-decomposed material, which is a biphasic intimate mixture of oxide and carbonate, yield information on the mechanism of decomposition and on the state of the solid during the decomposition itself.

Experimental

Solid solutions $Sr_xCa_{1-x}CO_3$ were obtained by mixing 2 *M* solutions of $Ca(NO_3)_2$ and $Sr(NO_3)_2$ in the desired proportions followed by dripping the solution into an excess of 2 *M* $(NH_4)_2CO_3$ solution at 90–95°C under conditions of vigorous stirring (*13*). Samples were prepared with 10 different Sr contents, corresponding notionally to x = 0.10, 0.20, 0.30, 0.40, 0.50, 0.60, 0.70, 0.80, and 0.90. All precipitates showed the pres-

ence of an orthorhombic phase with lattice parameters lying between those of aragonite and strontianite, depending on the composition (*13*).

Samples are designated for convenience according to the molar percentage Sr in the starting solution. Thus S40 signifies the $Sr_xCa_{1-x}CO_3$ sample with $x = 0.40$. For Sr concentrations of $x = 0.30$ and below, some pure calcite phase was also present. Thus the value of x is an underestimate in these cases.

Thermogravimetric (TG) analysis and quantitative DTA of all samples were performed in a coupled TG–DTA Mettler TA2000C apparatus in flowing gas (N_2 or CO_2) using samples of 12.5 mg and a heating rate of 20 K min^{-1}. The DTA apparatus was calibrated by using the melting of In and Al and the orthorhombic–rhombohedral phase transition of pure $SrCO_3$ (RPE, Carlo Erba) as calorimetric standards.

In addition to experiments carried to complete decomposition of the carbonate or to the instrumental limit (1573 K), a number of TG–DTA runs were made in which samples were heated in flowing CO_2 to an intermediate temperature and then cooled. To check for the occurrence of a phase transition, the cooled samples were then examined by X-ray powder diffraction using a CGR Theta 60 diffractometer with Cu$K\alpha$ radiation and a Ni filter. Lattice parameters were calculated using a program for the indexing of powder patterns and for the refinement of cell dimensions derived from an original version by Lindquist and Wengelin (*34*). The standard error in the determination of the parameters was lower than 0.15%.

A few other thermal analysis runs were carried out in an argon atmosphere and interrupted at an intermediate temperature where there had been partial decomposition. In this case, after cooling in argon, the partially decomposed sample was quickly transferred to a Lindemann capillary tube, sealed, and then subjected to Debye–Scherrer XRD analysis using a 114.6-mm Philips camera.

Results

General Characteristics in DTA and TG Analysis

The DTA traces recorded upon decomposition of $Sr_xCa_{1-x}CO_3$ solid solutions in nitrogen atmosphere are reported in Fig. 1. Three of these DTA curves, namely those for S10, S50, and S90, are also reproduced

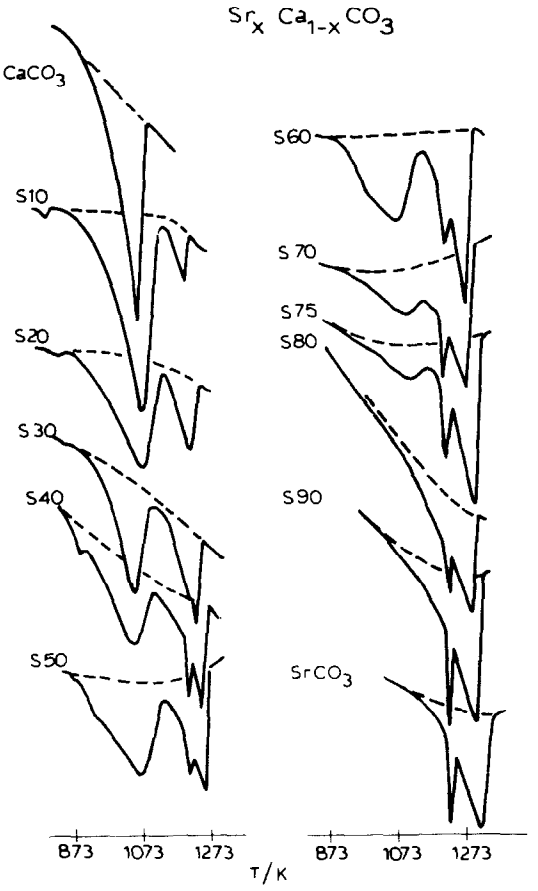

FIG. 1. DTA traces (endotherms) for solid solutions $Sr_xCa_{1-x}CO_3$ (designated as S100x) in flowing N_2. Experimental conditions: weight 12.5 mg, heating rate 20 K min^{-1}.

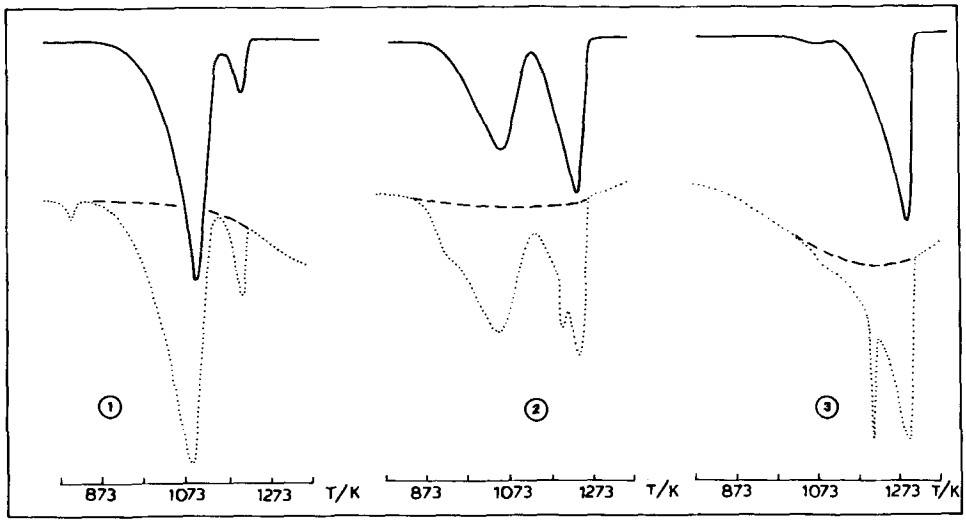

FIG. 2. Simultaneous DTG–DTA traces of solid solutions S10 (1), S50 (2), and S90 (3). —, DTG (weight losses). · · ·, DTA (endotherms).

on a rather larger scale in Fig. 2 together with the corresponding DTG traces recorded simultaneously. This discriminates clearly between the endotherms due to decomposition (i.e., coupled with weight losses) and those due to phase transitions.

It is clear from Figs. 1 and 2 that, as previously reported (*14*, *15*), the decomposition of the solid solutions carried out under these conditions occurs in two separate stages. These stages are represented by two prominent endothermic (and weight loss) peaks in the traces for all solid solutions except S80 and S90.

The loss of weight in the first and in the second stage roughly parallels the amounts of Ca^{2+} and Sr^{2+} present, respectively. Data for the first stage are shown in Fig. 3, where it is seen that the percentage weight loss decreases progressively with increasing molar percentage Sr (i.e., decreasing molar percentage Ca). However, close inspection of Fig. 3 at high molar percentage Sr indicates that the experimental points lie consistently below a strictly linear relation: in these cases the amount of carbonate ions decomposed in the first step is slightly lower than the Ca^{2+} concentration in the starting material.

The temperature of the second decomposition peak clearly increases with Sr concentration. Although not evident from Fig. 1, this is also the case for the first peak

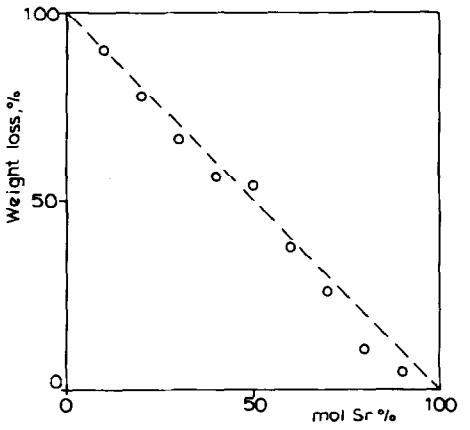

FIG. 3. Percentage of total weight loss in the first stage of decomposition in N_2 as a function of Sr content.

when physical factors such as the dilution of the decomposing component are taken into account (*15*).

Evidence for Phase Transitions

Comparison of the DTG and DTA traces in Fig. 2 reveals endotherms not accompanied by a weight loss. One is a small endotherm prior to or overlapping the first decomposition peak (S10 and S50), and the second, at higher temperature, is a pronounced sharp endotherm (S50 and S90).

By referring back to the full set of DTA curves in Fig. 1, it is evident that the first endothermic effect is observable as a shoulder on all samples up to S75, its temperature increasing with the Sr content. As regards the second effect, the sharp peak is observed with samples of Sr content from S30 upward, and in fact its temperature in all these cases is within the narrow range 1219–1224 K. These endotherms are due to phase transitions and will be referred to again later.

Evaluation of Heats of Decomposition

The total heat evaluated from the DTA traces is reported in Fig. 4a as a function of the composition. Neglecting for the moment the endothermic effects due to the phase transitions, an evaluation of the fraction of heat absorbed in the first and second decompositions, respectively, was made by assuming that the intermediate minimum in endothermicity could be taken as indicating the division between the two phenomena. The heat effects measured in this way are reported in Figs. 4b and 4c for the first and the second endotherm, respectively.

Heat evaluations of this kind are subject to appreciable error because on the one hand the baseline is affected by the variation in heat capacity during the whole transformation and on the other the gas evolving as a decomposition product may not equilibrate its energy before leaving the DTA cell. In order to obtain more reliable information on the variation of the heat effect with composition each experiment was repeated several times. The points in Fig. 4 are the average values obtained over the set of experiments. The error bars are a measure of the dispersion of the experimental data for each particular sample.

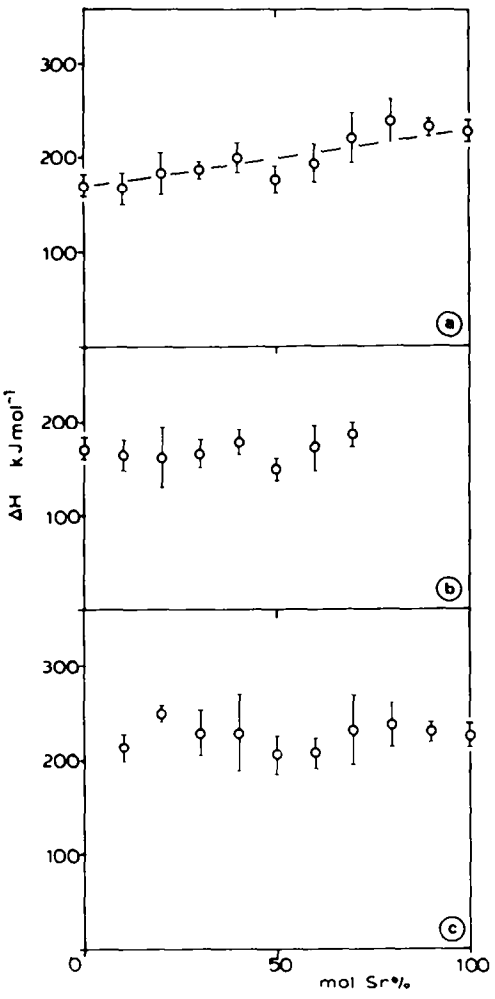

FIG. 4. Heat of decomposition of $Sr_xCa_{1-x}CO_3$ solid solutions in flowing N_2 (kJ absorbed per mole of carbonate unit decomposed) as a function of Sr content. (a) Total heat; (b) first decomposition peak; (c) second decomposition peak.

Despite experimental uncertainty and the neglect of the heat effect specifically associ-

ated with the phase transitions, Fig. 4a shows that the total heat absorbed increases progressively with increasing Sr content. The partial heat for the first decomposition profile (Fig. 4b) averages at 172 kJ/mole of evolved CO_2. This may be compared with the range 163–188 kJ mol^{-1} reported for the heat of decomposition of $CaCO_3$ (*21*). The partial heat for the second decomposition profile, inclusive of the phase transition, averages at 226 kJ/mole of evolved CO_2. This value is close to the range reported for decomposition of pure $SrCO_3$ (230–251 kJ mol^{-1}) (*21*).

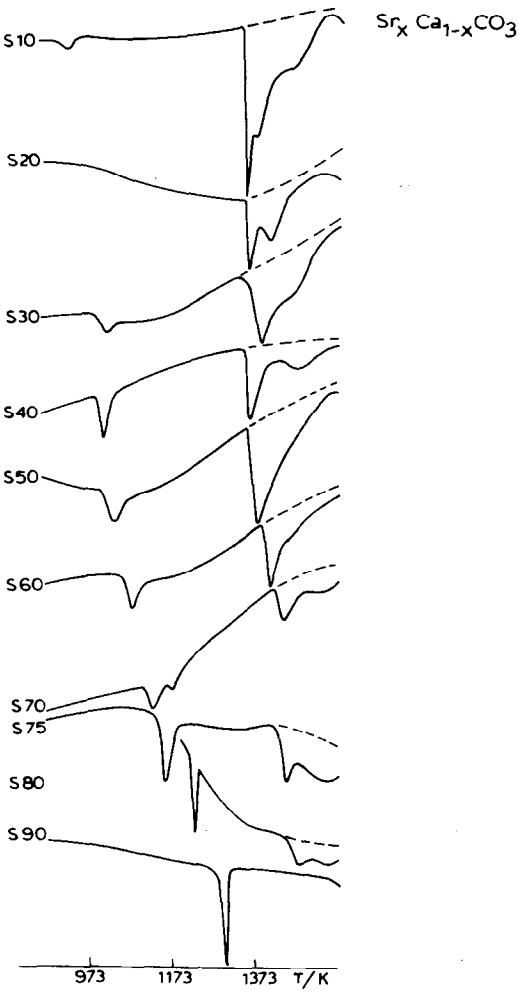

FIG. 5. DTA traces (endotherms) for solid solutions $Sr_xCa_{1-x}CO_3$ (designated as S100x) in flowing CO_2. Experimental conditions as in Fig. 1.

Thermal Behavior in CO_2 Atmosphere

By heating the solid solution samples in flowing CO_2 rather than in N_2, the onset of decomposition was displaced to higher temperatures. In this way the phase transition endotherms could be isolated from the decomposition endotherms and subjected to more detailed study.

Figure 5 illustrates the results obtained in this way. In all cases the onset of decomposition is shifted to temperatures above 1300 K, the percentage decomposition by 1573 K (the upper limit studied) decreasing with increasing Sr content, and the decomposition profile moving progressively to higher temperatures.

The TG curves corresponding to Fig. 5 were also measured, but for the sake of brevity are not reported. However, these curves clearly indicated that the first endotherm present in Fig. 5 (apparently unobserved in S20) was not accompanied by a weight loss, while the second endotherm was consistently accompanied by a weight loss, the DTG curves closely following the DTA traces.

The temperatures of the peaks of the phase transition endotherms of Fig. 5 are shown as a function of Sr content in Fig. 6. The temperature at which the transition takes place varies with composition and increases with Sr content. For samples up to and including S75 the temperature of the first DTA peak in Fig. 5 is the same as the temperature of the shoulder observed in the decomposition under N_2 in Fig. 1.

In order to check whether the first peak corresponded to a reversible or an irreversible phase transition, all samples were studied in a second type of DTA experiment in which they were first heated in CO_2 to a temperature just below the occurrence of any decomposition, cooled to room temper-

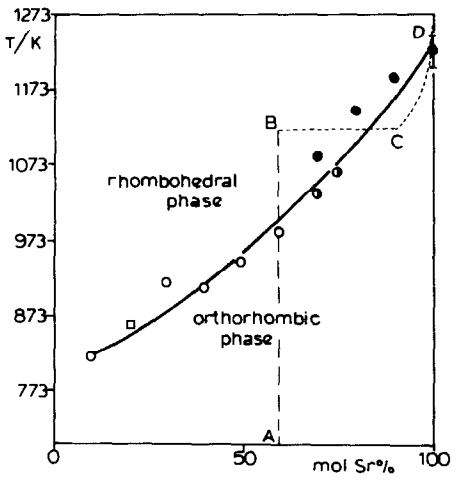

FIG. 6. The orthorhombic–rhombohedral phase transition in $Sr_xCa_{1-x}CO_3$ solid solutions in flowing CO_2. Temperature of the peak minimum (Fig. 5) as a function of Sr content. Empty circles, irreversible transformations; half-filled circles, partially reversible transformations; filled circles, reversible transformations; the squared point is taken from Fig. 1. For explanation of the dashed line ABCD, see text.

ature, and then reheated. For samples with Sr concentrations up to and including S60, the DTA curve observed during the reheating showed that the first peak had disappeared, thereby testifying that the transition was an irreversible one. For S80 and S90, on the other hand, the peak was still observed, showing that the transition in those cases was reversible. S70 and S75 showed an intermediate behavior. For S70, where there were two peaks, both were retained on reheating, but the lower temperature peak was reduced in intensity. In S75, the peak was also retained, but with a lower intensity. The irreversible transformations are reported as empty circles in Fig. 6, and the reversible ones as filled circles.

To confirm that the shoulder observed at low temperature in Fig. 1 upon heating in N_2 was associated with the same phase transition as is observed in CO_2, two samples, S40 and S60, were also submitted to the following DTA experiment. They were first heated in CO_2 to just below the temperature at which their decomposition would have begun; they were then cooled down in CO_2 to room temperature and reheated in nitrogen. In both cases, the shoulder clearly visible in Fig. 1 for S40 and S60 at 817 K and 918 K, respectively, had disappeared.

X-Ray Diffraction Studies after Thermal Treatment

The results in the preceding sections indicate that the first endothermic peak visible in CO_2, as well as the shoulder visible in N_2, correspond to the same phase transition. In order to identify the phases involved, samples heated in CO_2 to a temperature intermediate between the phase transition and decomposition were cooled and submitted to XRD analysis. Apart from the calcite impurity present in S10, S20, and S30, which did not undergo any modification, in all samples with a strontium content equal to or below S60, X-ray analysis showed that a transformation of the orthorhombic strontianite–aragonite phase to a rhombohedral phase had occurred. In S80, S90, and pure $SrCO_3$, on the other hand, the initial orthorhombic phase was identified with no detectable changes in comparison with the starting material. With S70 both orthorhombic and rhombohedral phases were found to be present after the cooling to room temperature. The values of the *a* and *c* parameters of the hexagonal unit cell corresponding to the rhombohedral structure are reported as a function of the composition in Fig. 7. These values increase with Sr content.

Similar experiments on samples heated in N_2 or other inert gas to partial decomposition (e.g., heated only to the end of the first decomposition stage) are less easy to perform, because of the high reactivity to water vapor of the oxide phase produced in the first decomposition stage. However, a successful experiment was achieved with

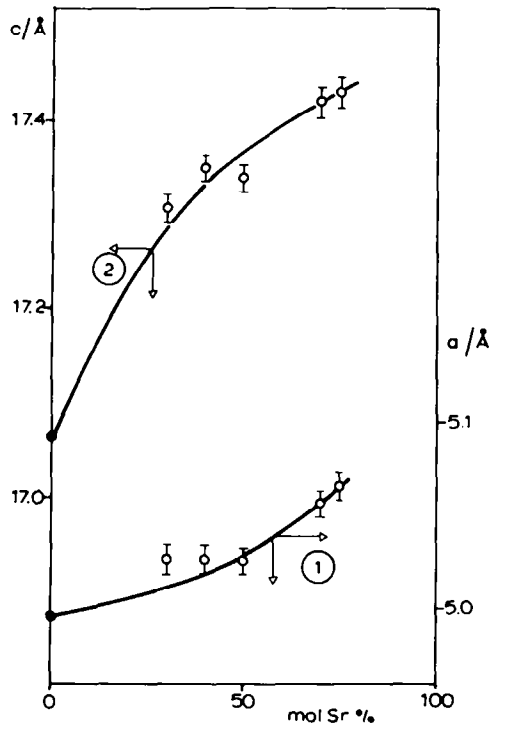

FIG. 7. Lattice parameters a (1) and c (2) for the hexagonal cell corresponding to the rhombohedral solid solutions as a function of Sr content. Filled circles are reference values for pure calcite (*21*).

S60. The solid was heated in argon to the temperature where the first decomposition stage was complete and was then cooled to room temperature: the partially decomposed sample was quickly introduced into a Lindemann tube and examined by the Debye–Scherrer method (*14*). The sample was multiphasic but the presence of an orthorhombic phase was diagnosed, albeit with rather diffuse reflections. The lattice parameters corresponded to a $Sr_xCa_{1-x}CO_3$ phase with a strontium content of about 90 mole%.

Evaluation of the Heat of Phase Transition

The heats related to the orthorhombic–rhombohedral phase transition in CO_2 are reported in Fig. 8 as a function of composition. These heats can be estimated with much more precision than the decomposition heats because of the lower variation in heat capacity and the absence of any evolution of gas. They increase strikingly with strontium content.

It was also possible in the DTA experiments carried out in N_2 to estimate from the data in Fig. 1 the heat of the phase transition for the samples with $x = 0.4$ and above. In Fig. 9 the heats of the phase transition per mole of undecomposed carbonate remaining at the temperature of the transition (peak maximum at 1220 K) are reported. The TG data enabled this amount of carbonate to be quantified.

Discussion

A. Decomposition

It has already been reported (*2–10, 12, 14, 15*) that solid solutions of alkaline earth carbonates often exhibit a two-stage decomposition pattern in CO_2 atmosphere. In the first stage the cations demix, forming

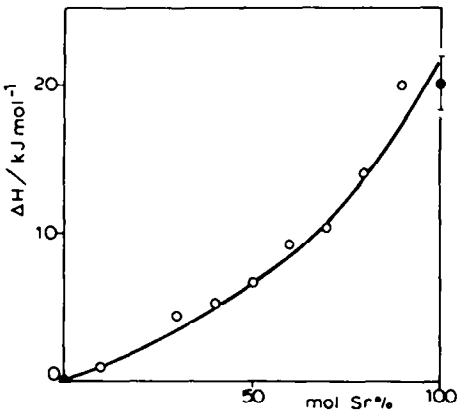

FIG. 8. ΔH of transition (kJ per mole of carbonate unit) as a function of Sr content for the orthorhombic–rhombohedral phase transition in $Sr_xCa_{1-x}CO_3$ solid solutions in flowing CO_2. Filled circles refer to published data for pure strontianite (*28*) and pure aragonite (*38*).

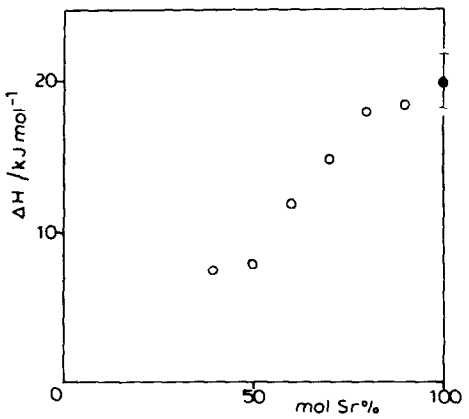

FIG. 9. ΔH of transition (kJ per mole of undecomposed carbonate, measured by TG) as a function of composition for the orthorhombic–rhombohedral phase transition in $Sr_xCa_{1-x}CO_3$ solid solutions partially decomposed in flowing N_2. The filled circle refers to published data for pure strontianite (*28*).

two well-dispersed phases, one phase of which is basically the oxide of the component with the less stable carbonate and the other phase the carbonate of the other component. The second stage represents the decomposition of this carbonate, and except for the Mg–Ca system it is accompanied by facile remixing of cations into a single-oxide phase. Figure 5 shows evidence of this two-stage decomposition in CO_2 atmosphere for the $Sr_xCa_{1-x}CO_3$ solid solutions studied in this work. The first stage begins at about 1250 K for the more Ca-rich solid solutions. There is an additional initial feature affecting the endotherm for S10 and S20 (accompanied by a loss of weight) which is an anomaly caused by the presence of a significant content of calcite impurity in these samples.

$Sr_xCa_{1-x}CO_3$ solid solutions exhibit a clear two-stage decomposition also in inert gas atmosphere (Fig. 1), and differ in this respect from the reported behavior of dolomite (*2–10, 14*).

In both atmospheres tested the temperature of onset of the decomposition of $Sr_xCa_{1-x}CO_3$ increases with the Sr content. The results in CO_2 atmosphere clearly show this trend in the high-temperature range. The behavior is evident in N_2 atmosphere provided the influence of the amount of decomposing component on the DTA measurement is taken into account (*15*). Thus the Sr^{2+} cations exert a significant effect on the stability of the whole solid solution, hindering the release of CO_2 also from the environment of the Ca^{2+} cations. Other results are in good agreement with this deduction. For instance, the loss of weight at the end of the first peak in nitrogen is often lower than that corresponding to the decomposition of the amount of $CaCO_3$ present in the solid solution, especially at high Sr content (Fig. 3). Moreover, the XRD analysis of the S60 sample submitted to partial decomposition shows that at the end of the first peak the carbonate present exhibits lattice parameters characteristic of Ca-containing $SrCO_3$, although richer in Sr than the starting material.

The temperature of decomposition of the intermediate Sr-rich carbonate phase decreases with increasing Ca content (Fig. 1). This temperature shift indicates a high reactivity of the carbonate phase derived from the partial decomposition of the starting solid solution. The high reactivity of the intermediate carbonate phase is confirmed by the easy remixing of the cations to form a single-oxide phase when this carbonate decomposes. The diffuseness of the XRD lines for the partially decomposed S60 sample is also in line with this. However, the dilution of the intermediate carbonate in a matrix of oxide, with a consequent decrease in local CO_2 pressure, may also contribute to the lowering of the decomposition temperature.

Notwithstanding the retention of some Ca in the intermediate carbonate phase, the weight losses and the heat effects measured in the two-stage decomposition in N_2 accord well with the preferential formation of

CaO as a separate phase and of a Sr-enriched carbonate solid solution as the other phase in the first stage, the second stage corresponding to the decomposition of this latter carbonate. The endothermic effects of the first and second peaks measured separately (Figs. 4b and 4c) are close to the heat of decomposition of pure $CaCO_3$ and $SrCO_3$, respectively.

The deviation from linearity of Fig. 4a as well as the minimum in the middle range of composition of Figs. 4b and 4c might be taken as an indication of thermal effects due to the heat of mixing and to a nonideality of the solid solution itself. The magnitude of these heat effects, however, falls in the range of the standard error expected for quantitative DTA measurements in our conditions (~20 kJ mol^{-1}).

B. Phase Transitions

As already indicated under Introduction, both end members, $CaCO_3$ and $SrCO_3$, undergo a phase transition from orthorhombic to rhombohedral structure. In the case of $CaCO_3$, while aragonite (orthorhombic) is metastable the thermodynamically stable phase at room temperature is calcite (rhombohedral). The transition aragonite–calcite occurs irreversibly at 700–1000 K (*25*). Strontianite, the orthorhombic polymorph of $SrCO_3$, is the thermodynamically stable phase at room temperature and undergoes a transition to a rhombohedral form at about 1200 K (*35*). In this case the transition is reversible.

The results in Figs. 1 and 5 show that in the orthorhombic solid solutions this kind of transition always occurs, with characteristics determined by the mutual amounts of Ca^{2+} and Sr^{2+}. The heat relating to the phase transition increases with strontium content (Fig. 8) and accordingly the transition takes place at higher temperature (Figs. 1, 5, and 6). However, the variation of the ΔH value with strontium content departs from linearity, suggesting perhaps that there is an influence of cation disorder superimposed on the composition effect.

As far as reversibility is concerned, both XRD and DTA data indicate that as long as the Sr content is below 70% the transition is irreversible; i.e., the role of Ca^{2+} prevails and the rhombohedral solid solution is stable also at room temperature. From 80% Sr upward the transition is completely reversible, as in pure $SrCO_3$. The intermediate compositions (S70 and S75) show a mixed behavior with evidence of partial reversibility. For each composition examined the phase transition temperature (Fig. 6) falls in the interval between the occurrence of orthorhombic and rhombohedral phases reported by Chang (*32*) on the basis of equilibrium solid state reactions. The rhombohedral solid solutions show an increase in lattice parameters upon substitution of Ca by Sr, as expected.

The phase transition superimposed on the second decomposition stage when samples are heated in N_2 is also an orthorhombic–rhombohedral transition. It occurs at the same temperature in all cases examined (peak maximum at about 1220 K). To understand this phenomenon it must be taken into account that, after the first phase transition, the enrichment in Sr of the carbonate phase during the first decomposition brings the system into the range of stability of the orthorhombic phase, i.e., below the curve defined by the transition temperatures in Fig. 6. Thus the carbonate phase decomposing in the second stage is an orthorhombic one, which undergoes again the transition to the rhombohedral structure alongside decomposition (Fig. 1). To illustrate this further Fig. 6 reports as a dashed line the path followed by S60 during decomposition. From point A to point B upon heating the orthorhombic–rhombohedral transition occurs. The first decomposition leaves an orthorhombic carbonate phase enriched in strontium, as indicated by XRD analysis (point C in Fig. 6, below

the phase transition curve). Upon further heating a phase transition will again occur (line C–D). The temperature of this latter phase transition does not vary with the composition of the starting material nor does it differ significantly from the transition temperature of pure strontianite.

It is interesting to note that the heat related to this phase transition, measured per mole of undecomposed material (shown in Fig. 9), is sensitive to the initial composition, and is lower the higher the initial Ca content. As the features of the transition (shape, peak temperature, etc.) are the same in all samples, a possible explanation is that the molar heat of transition is actually the same, but that some of the residual carbonate is too disordered to exhibit the transition. The production of amorphous material during thermal decomposition of carbonates has been previously reported (*5, 36*) and $CaCO_3$ in amorphous form can be obtained by recarbonation of CaO (*37*). It is very likely that in partially decomposed $Sr_xCa_{1-x}CO_3$ the noncrystalline fraction is higher the greater the Ca content in the starting material, i.e., in the fraction already decomposed.

Conclusions

The occurrence of a two-stage decomposition in the thermal transformation of $Sr_xCa_{1-x}CO_3$ into $Sr_xCa_{1-x}O$ solid solutions has been confirmed in the whole range of composition. This decomposition path yields in the intermediate range a disordered two-phase system (composed of a Ca-rich oxide phase and a Sr-rich carbonate phase) including finely divided poorly crystalline or amorphous material.

The temperatures at which the two respective decompositions occur depend upon the initial composition and the CO_2 pressure.

On heating in CO_2 an orthorhombic–rhombohedral phase transition occurs in the whole range of composition examined, yielding a continuous series of rhombohedral solid solutions. The temperature at which the transition occurs as well as the heat involved in the transition itself vary with composition. The transition is irreversible up to a Sr/(Ca + Sr) ratio of 0.6. Above this value it becomes progressively reversible as in pure strontianite.

Acknowledgments

We thank Dr. M. M. Ramirez de Agudelo for help with the preparation and structural characterization of the carbonates. We acknowledge the support of this work by a NATO Research Grant.

References

1. R. J. REEDER (Ed.), "Carbonates in Mineralogy and Chemistry," Mineralogical Society of America (1983).
2. D. A. YOUNG, "Decomposition of Solids," Pergamon, Oxford (1966).
3. W. E. BROWN, D. DOLLIMORE, AND A. K. GALWEY, *in* "Chemical Kinetics" (C. H. Bamford and C. F. H. Tipper, Eds.), Vol. 22, p. 241, Elsevier, Amsterdam (1980).
4. W. R. BANDI AND G. KRAPF, *Thermochim. Acta* **14,** 221 (1976).
5. E. K. POWELL AND A. W. SEARCY, *J. Amer. Ceram. Soc.* **61,** 216 (1978).
6. H. HASHIMOTO, E. KOMAKI, F. HAYASHI, AND T. UMATSU, *J. Solid State Chem.* **33,** 181 (1980).
7. H.-G. WIEDEMANN AND G. BAYER, *Thermochim. Acta* **38,** 109 (1980).
8. G. SPINOLO AND D. BERUTO, *J. Chem. Soc. Faraday Trans. 1* **78,** 2631 (1982).
9. G. SPINOLO AND V. ANSELMI TAMBURINI, *Z. Naturforsch. A* **39,** 975, 981 (1984).
10. R. OTSUKA, *Thermochim. Acta* **100,** 69 (1986).
11. M. M. EVSTIGNEEVA, N. A. IOFIS, AND A. A. BUNDEL, *Zh. Fiz. Khim.* **48,** 1360 (1974).
12. D. J. MORGAN AND A. E. MILODOWSKI, *in* "Thermal Analysis" (B. Miller, Ed.), p. 642, Wiley, Chichester (1982).
13. M. M. RAMIREZ DE AGUDELO, Thesis, University of Bath (1980); M. M. RAMIREZ DE AGUDELO AND F. S. STONE, *Mater. Sci. Monogr.* **10,** 695, Elsevier, Amsterdam (1982).
14. B. FUBINI AND F. S. STONE, *Mater. Sci. Monogr.* **28,** 85, Elsevier, Amsterdam (1985).

15. B. FUBINI, F. DI RENZO, AND F. S. STONE, *Thermochim. Acta* **122,** 23 (1987).
16. M. D. JUDD AND M. I. POPE, *Thermochim. Acta* **7,** 248 (1973).
17. A. RELLER, C. PADESTE, AND P. HUG, *Nature (London)* **329,** 527 (1987).
18. J. M. CRIADO, F. GONZALEZ, AND J. MORALES, *Thermochim. Acta* **32,** 99 (1979).
19. J. M. CRIADO, F. ROUQUEROL, AND J. ROUQUEROL, *Thermochim. Acta* **38,** 109 (1980).
20. M. MACIEJEVSKI AND J. BALDYGA, *Thermochim. Acta* **92,** 108 (1985).
21. S. GAL, G. POKOL, AND E. PUNGOR, *Thermochim. Acta* **16,** 339 (1976).
22. Z. N. ZEMTSOVA, M. M. PAVLYUCHENKO, AND E. A. PRODAN, *Vesti Akad. Navuk BSSR, Ser. Khim. Navuk,* 21 (1971).
23. M. M. PAVLYUCHENKO, E. A. PRODAN, Z. M. ZEMTSOVA, AND Y. V. ZONOV, *Russ. J. Phys. Chem.* **47,** 1090 (1973).
24. J. A. SPEER, *in* "Carbonates in Mineralogy and Chemistry" (R. J. Reeder, Ed.) p. 145, Mineralogical Society of America (1983).
25. W. D. CARLSON, *in* "Carbonates in Mineralogy and Chemistry" (J. Reeder, Ed.), p. 191, Mineralogical Society of America (1983).
26. T. L. WEBB AND J. E. KRUGER, "Differential Thermal Analysis," Vol. 1, "Fundamental Aspects" (R. C. MacKenzie, Ed.), p. 303, Academic Press, New York/London (1970).
27. C. N. R. RAO AND P. N. MEHROTRA, *Bull. Mater. Sci.* **2,** 67 (1980).
28. R. POMPE, *Thermochim. Acta* **20,** 229 (1977).
29. K. IWAGUCHI, C. WATANABE, AND R. O. OTSUKA, *Thermochim. Acta* **64,** 381 (1983).
30. E. P. OSTAPCHENKO, *Izv. Akad. Nauk SSSR, Ser. Fiz.* **20,** 1105 (1956).
31. H. D. HOLLAND, M. BORCSIK, J. MUNOZ, AND U. M. OXBURGH, *Geochim. Cosmochim. Acta* **27,** 957 (1963).
32. L. L. Y. CHANG, *J. Geol.* **73,** 346 (1965).
33. W. D. CARLSON, *Amer. Mineral.* **65,** 1252 (1980).
34. O. LINDQUIST AND F. WENGELIN, *Ark. Kemi* **28,** 179 (1967).
35. E. RAPOPORT AND C. W. F. T. PISTORIUS, *J. Geophys. Res.* **72,** 6353 (1967).
36. H.-G. WIEDEMANN AND G. BAYER, *Thermochim. Acta* **121,** 479 (1987).
37. M. MACIEJEVSKI AND A. RELLER, private communication.
38. P. A. ROCK AND A. Z. GORDON, *J. Amer. Chem. Soc.* **98,** 2364 (1976).